

Advanced Quantum Annealing for the Bi-Objective Traveling Thief Problem: An ε -Constraint-based Approach

Nguyen Hoang Viet, Nguyen Xuan Tung, Trinh Van Chien, Member, IEEE,
and Won-Joo Hwang, Senior Member, IEEE

Abstract—This paper addresses the Bi-Objective Traveling Thief Problem (BI-TTP), a challenging multi-objective optimization problem that requires the simultaneous optimization of travel cost and item profit. Conventional methods for the BI-TTP often face severe scalability issues due to the complex interdependence between routing and packing decisions, as well as the inherent complexity and large problem size. These difficulties render classical computing approaches increasingly inapplicable. To tackle this, we propose an advanced hybrid approach that combines quantum annealing (QA) with the ε -constraint method. Specifically, we reformulate the bi-objective problem into a single-objective formulation by restricting the second objective through adjustable ε -levels, determined within established upper and lower bounds. The resulting subproblem involves a sum of fractional terms, which is reformulated with auxiliary variables into an equivalent form. Subsequently, the equivalent formulation is transformed into a Quadratic Unconstrained Binary Optimization (QUBO) model, enabling direct solution via a quantum annealing (QA) solver. The solutions obtained from the quantum annealer are subsequently refined using a tailored heuristic procedure to further enhance overall performance. By leveraging the flexibility in selecting ε parameters, our approach effectively captures a broad Pareto front, enhancing solution diversity. Experimental results on benchmark instances demonstrate that the proposed method effectively balances two objectives and outperforms baseline approaches in time efficiency.

Index Terms—Quantum Annealing, Multi-objective Optimization, Travelling Thief Problem, QUBO model

Nguyen Hoang Viet and Trinh Van Chien are with the School of Information and Communications Technology, Hanoi University of Science and Technology, Hanoi 100000, Vietnam (e-mail: viet.nh220050@sis.hust.edu.vn and chientv@soict.hust.edu.vn). Nguyen Xuan Tung is with the Faculty of Interdisciplinary Digital Technology, PHENIKAA University, Yen Nghia, Ha Dong, Hanoi 10000, Viet Nam (email: tung.nguyenxuan@phenikaa-uni.edu.vn). Won-Joo Hwang is with the School of Computer Science and Engineering, Center for Artificial Intelligence Research, Pusan National University, Busan 46241, South Korea (e-mail: wjh-wang@pusan.ac.kr). This work was supported in part by BK21 FOUR, Korean Southeast Center for the 4th Industrial Revolution Leader Education; in part by the Institute of Information & communications Technology Planning & Evaluation (IITP) under the Artificial Intelligence Convergence Innovation Human Resources Development (IITP-2025-RS-2023-00254177) grant funded by the Korea government(MSIT); in part by Quantum Computing based on Quantum Advantage challenge research(RS-2024-00408613) through the National Research Foundation of Korea(NRF) funded by the Korean government (Ministry of Science and ICT(MSIT)); in part by Creation of the quantum information science R&D ecosystem(based on human resources) (Agreement Number) through the National Research Foundation of Korea(NRF) funded by the Korean government (Ministry of Science and ICT(MIST)) (RS-2023-00256050); and in part by the National Research Foundation of Korea(NRF) grant funded by the Korea government(MSIT)(RS-2024-00336962). Corresponding author: Won-Joo Hwang.

I. Introduction

A substantial class of real-world combinatorial optimization problems is NP-hard, making it computationally challenging to find an optimal solution through conventional approaches such as branch-and-bound [1] and dynamic programming [2]. To circumvent this limitation, heuristic approaches are commonly employed [3]–[5], which, however, require a trade-off between computational efficiency and solution quality. Additionally, real-world problems often exhibit two intertwined characteristics: harsh complexity and interdependent objectives [6]. These features give rise to multi-objective optimization problems (MOPs), where objectives are often in conflict. In such settings, a single solution that optimizes all objectives simultaneously rarely exists. Consequently, solutions are evaluated based on Pareto dominance [7], where a solution is considered to dominate another if it is no worse in all objectives and strictly better in at least one. The goal in solving MOPs is to approximate the Pareto front: a set of non-dominated solutions that represent the best trade-offs among objectives.

Many scalarization techniques, such as the weighted-sum method [8] and the ε -constraint method [9], have been developed to address multi-objective optimization problems (MOPs). These methods typically convert a MOP into a series of single-objective problems, which are then solved individually to yield high-quality solutions. While the weighted-sum method is limited in its ability to capture non-convex regions of the Pareto front and does not offer control over the solution's position along the front [10], the ε -constraint method is highly dependent on the careful selection of the ε -levels [11]. Naive selection can result in infeasible subproblems or poor coverage of the Pareto front. Besides scalarization methods, an alternative and promising approach for MOPs is the use of Multi-Objective Evolutionary Algorithms (MOEAs), due to their ability to simultaneously handle nonlinear, nondifferentiable, and combinatorial objectives within an efficient time [12]. Despite their flexibility and robustness, MOEAs often demand a substantial number of function evaluations to converge toward a satisfactory approximation, leading to high computational overhead.

Quantum computing has emerged as a promising paradigm for solving combinatorial optimization problems. Existing approaches can be grouped into three categories based on hardware implementation: (i) purely quantum algorithms that run exclusively on quantum hardware

[13], [14]; (ii) quantum-inspired heuristics executed on classical machines [15], [16]; and (iii) hybrid methods combining quantum and classical resources [17], [18]. Due to the hardware limitations of the noisy intermediate-scale quantum (NISQ) era, hybrid approaches are generally preferred, as they leverage both quantum processing units (QPUs) and state-of-the-art classical solvers for improved scalability in large-scale applications. Among these approaches, hybrid QA stands out due to its practical implementation on the D-Wave quantum annealer [19] and its seamless integration with classical optimization techniques via the D-Wave Hybrid Solver Service. In this work, we conduct experiments with hybrid QA using the D-Wave Hybrid Solver. This solver is capable of solving constrained quadratic optimization problems with up to 500,000 binary variables and 100,000 linear or quadratic constraints. With the support of D-Wave hardware, QA has been demonstrated to achieve superior performance over classical baselines in optimizing single-objective combinatorial problems [20]–[22]. Motivated by these results, we seek to extend this powerful computational paradigm for more challenging scenarios, when the problem are formulated as multi-objective optimization problems. In this work, the BI-TTP is adopted as the case study to evaluate the effectiveness of our proposed approach.

The TTP [23] is a well-known benchmark that exemplifies the challenges of multi-objective combinatorial optimization. It integrates two classical NP-hard problems, the Traveling Salesman Problem (TSP) and the Knapsack Problem (KP), into a single unified framework. In the TTP, a thief must visit each city exactly once while selecting items of varying value and weight to maximize total profit. However, carrying more items slows down travel speed, creating a conflict between minimizing tour time and maximizing knapsack profit. A faster route limits item collection, while higher profits often require longer travel times. However, several challenges arise when applying QA directly to multi-objective problems such as the BI-TTP. The first limitation is that QA produces only a single solution per execution, necessitating multiple runs to approximate the Pareto front. Consequently, the solution quality may deteriorate if QA repeatedly produces identical solutions. The second challenge lies in the dynamic covariance among objectives, which can significantly degrade the performance of QA if the interference of each objective is not carefully regulated. Under such circumstances, the solution produced by QA may be biased toward a limited region of the objective space, thereby failing to capture the full range of values represented in the true non-dominated solution set.

Motivated by the aforementioned challenges, this work introduces a novel quantum annealing-based approach for solving the bi-objective Traveling Thief Problem (BI-TTP), specifically under the setting where item value depreciation is omitted. This assumption aligns with the formulations adopted in the BI-TTP competitions held

at the EMO-2019¹ and GECCO-2019² conferences. Our method employs the ε -constraint technique to transform the bi-objective formulation into a single-objective problem, wherein one objective is optimized while the other is bounded by a tunable threshold within predefined upper and lower limits. To exploit the computational advantages of quantum computing, the resulting problem is further reformulated as a QUBO model, enabling direct solution via D-Wave’s quantum annealer. A custom-designed heuristic is then applied to refine the raw solutions returned by the quantum hardware. To the best of our knowledge, our method represents the first work to apply quantum computing techniques to solve either the single- or bi-objective variant of the Traveling Thief Problem. The main contributions of this work are summarized as follows:

- We propose a novel hybrid approach that combines quantum annealing with the ε -constraint method to the traveling thief problem, where the total item profit is incorporated as a constraint bounded by a tunable threshold. By systematically varying this threshold, we repeatedly minimize the travel cost under different profit constraints, enabling effective exploration of the Pareto front.
- The reformulated single objective problem involves a sum of fractional quadratic terms, which cannot be directly solved using the QA solver. To address this, we propose an iterative transformation technique to handle fractional quadratic terms by reformulating the objective into a difference of quadratic expressions. The resulting problem is then expressed as a QUBO model and efficiently solved using D-Wave’s quantum annealer, leveraging the capabilities of quantum annealing to handle large-scale combinatorial optimization.
- To enhance the solutions obtained from D-Wave’s quantum annealer, we develop a heuristic refinement procedure that adjusts the item selection. This post-processing step improves solution quality and promotes better convergence toward the Pareto front.
- Finally, we evaluate our approach on the synthetic dataset from [24], which features three distinct item weight distributions: bounded strongly correlated, uncorrelated, and uncorrelated similar weight. In all categories, our approach consistently outperforms state-of-the-art classical algorithms including MOEA/D [25], NSGA-II [26], and U-NSGA-III [27] in computational efficiency. Specifically, our approach achieves up to an 9× reduction in runtime on the bounded strongly correlated instances.

The remainder of this paper is organized as follows. The related works are discussed in Section II Section III provides a detailed description of the bi-objective Traveling Thief Problem (BI-TTP), along with an illustrative example highlighting its constraints and inherent complexity. Section IV presents the overall framework of our proposed

¹<https://www.egr.msu.edu/coinlab/blankjul/emo19-thief/>

²<https://www.egr.msu.edu/coinlab/blankjul/gecco19-thief/>

approach, which integrates the ε -constraint method with quantum annealing to solve the BI-TTP. In Section V, we detail the transformation process that reformulates the original problem into a quadratic expression compatible with quantum annealing. Numerical results and performance evaluations are presented in Section VI, followed by concluding remarks in Section VII.

II. Related Works

The Traveling Thief Problem. The TTP was first introduced in [23], offering a more sophisticated and realistic formulation than the traditional TSP. The TTP is typically formulated in two main variants: a single-objective version (TTP1) and a bi-objective version (TTP2), also referred to as BI-TTP, which serves as the primary focus of this study. The single-objective version (TTP1) combines both objectives into a single fitness function and has been the primary focus of existing researches [28]–[30]. In contrast, the bi-objective version (TTP2 or BI-TTP) treats travel time and item value as separate objectives, aiming to determine a set of Pareto-optimal solutions that reveal the trade-off between time and profit. While the original TTP2 formulation in [23] assumes that item values decay over time, this temporal degradation was removed in a later variant proposed in [31]. Despite its practical relevance, the BI-TTP has received comparatively less attention in the literature. Some studies have attempted to address this gap. For instance, the authors in [32] proposed a multi-objective approach to jointly optimize the travel path and item selection, demonstrating solution improvements over single-objective approaches. Similarly, [33] employed dynamic programming to identify optimal packing strategies for fixed routes, while [34] introduced a specialized multi-objective variant of NSGA-II to approximate the Pareto front. Despite these efforts, existing approaches rely entirely on classical computing paradigms, which struggle with the combinatorial explosion of possibilities inherent in TTP, especially in the bi-objective case. These techniques remain computationally expensive when applied to large-scale or time-sensitive instances, thereby limiting their practical utility.

Quantum Annealing for Combinatorial Optimization problems. Quantum annealing (QA) has increasingly been recognized as a powerful alternative to classical algorithms for solving NP-hard combinatorial optimization problems across various domains. In finance, [35] employed reverse quantum annealing (reverse QA), which integrates both forward and reverse annealing processes to bypass local minima, on the D-Wave 2000Q processor to address the portfolio optimization problem. Nevertheless, hardware constraints restrict its applicability to small-scale instances with at most 64 binary variables. In the transportation and logistics domain, QA has also been applied to the air traffic control problem by discretizing delay times into incremental levels and assigning a binary variable to each level to construct a QUBO formulation [36]. For urban mobility problems, QA has been utilized with manually tuned penalty constraints

to prioritize particular assignment decisions [20]. Furthermore, [21] showed that QA significantly outperforms standard mixed-integer linear programming in deep space network scheduling, handling real-world requests much faster. Recent advancements have continued to expand QA’s utility: [22] combined QA with Simulated Annealing to refine solutions for maximum independent set problems, while [37] demonstrated that hybrid QA models can match the accuracy of state of the art classical solvers across more than 50 different NP-hard problems at substantially faster computation time. Additionally, by utilizing a preprocessing protocol to condense network sizes in facility location problems, [38] reduced the required binary variables, thereby expanding the scale of models that can be solved.

For multi-objective scenarios, [39] adopted a weighted-sum approach to combine multiple objectives into a single objective function and then obtained solutions through QUBO transformation. However, the weighted-sum method frequently experiences performance drops when dealing with complex intrinsic interference among objectives, primarily because selecting appropriate weights is highly challenging [10]. In contrast, our approach effectively manages this conflict by imposing strict limits on the values an objective can obtain.

The classical Traveling Salesman Problem (TSP) has also been efficiently solved using QA, as reported in [40]. More recently, QA has been adapted to the more complex Steiner Traveling Salesman Problem (STSP) by integrating a classical method to filter out unnecessary or costly path distances [41]. Nevertheless, its more challenging variant, the Traveling Thief Problem (TTP), has not yet been addressed using QA. This limitation arises because the TTP objective function contains fractional quadratic terms, which cannot be directly solved by QA. In this work, we overcome this limitation by introducing a conversion approach that transforms the TTP objective into an equivalent QUBO formulation suitable for QA.

III. Description of the BI-TTP

In the BI-TTP, a thief must visit a set of N cities $\{c_1, c_2, \dots, c_N\}$, forming a Hamiltonian cycle. The distance between any two cities c_u and c_v is represented by $d_{u,v}$. The knapsack component is integrated into the problem by associating each city c_i with a set of items B_i . The k -th item $\text{item}_{i,k} \in B_i$ has an associated profit $p_{i,k}$ and weight $w_{i,k}$. The thief starts and ends the tour at the city c_1 , and may collect items at any intermediate city c_2, \dots, c_N , subject to a knapsack capacity constraint W . That is, the total weight of all selected items must not exceed W . Although collecting items increases total profit, it also reduces the thief’s travel speed due to the added weight. When the knapsack is empty, the thief travels at maximum speed v_{\max} ; when fully loaded, the speed drops to a minimum value v_{\min} .

Let the traveling strategy be denoted by $\mathcal{A} = \{\alpha_1, \alpha_2, \dots, \alpha_N\}$, where $\alpha_1 = 1$ and $(\alpha_2, \dots, \alpha_N)$ is a permutation of the set $\{2, 3, \dots, N\}$, representing the

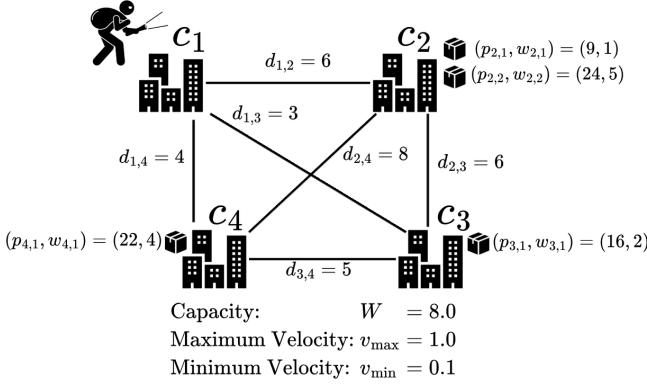


Fig. 1: A four-city BI-TTP instance: To complete the tour in the minimum time, the thief can follow the route $c_1 \rightarrow c_3 \rightarrow c_2 \rightarrow c_4 \rightarrow c_1$ without collecting any items. Conversely, to maximize profit, the thief must collect items $\text{item}_{2,1}$, $\text{item}_{2,2}$, and $\text{item}_{3,1}$, and travel along the route $c_1 \rightarrow c_4 \rightarrow c_2 \rightarrow c_3 \rightarrow c_1$ to complete the tour in the shortest possible time.

remaining $N - 1$ cities. In other words, c_{α_i} is the i -th city the thief travels in the tour. To facilitate understanding, we also define $c_{\alpha_{N+1}} = c_1$, indicating that the $(N + 1)$ -th city in the tour is the same as the starting city c_1 . Besides, we denote picking strategy $\mathcal{Z} = \{z_{i,k} \in \{0, 1\} \mid k = \overline{1, |B_i|}\}$, in which $z_{i,k} = 1$ if the thief collects the k -th item located in the city c_i , and $z_{i,k} = 0$, otherwise. Along with this notation, the weight of the knapsack after visiting the city c_{α_i} can be calculated as

$$W_i = \sum_{j=1}^i \sum_{k=1}^{|B_{\alpha_j}|} w_{\alpha_j, k} z_{\alpha_j, k}, \forall i = \overline{1, N}. \quad (1)$$

where $w_{\alpha_j, k}$ is the weight of the k -th item at the city α_j . Since items cannot be discarded once collected, the cumulative weight of selected items does not decrease throughout the entire tour. Therefore, we have $W_1 \leq W_2 \leq \dots \leq W_N$. Additionally, the thief must ensure that the total weight of collected items does not exceed the knapsack capacity W . Thus, the capacity constraint of the BI-TTP is represented by

$$W_N \leq W. \quad (2)$$

Consequently, the thief's velocity when traveling from city c_{α_i} to city $c_{\alpha_{i+1}}$ is given by

$$v_{i,i+1} = v_{\max} - W_i/W (v_{\max} - v_{\min}), \quad (3)$$

This velocity reflects the trade-off between collecting items and minimizing travel time. Then, the time required to travel from city c_{α_i} to city $c_{\alpha_{i+1}}$ can be computed as

$$t_{i,i+1} = \frac{d_{\alpha_i, \alpha_{i+1}}}{v_{i,i+1}} = \frac{d_{\alpha_i, \alpha_{i+1}}}{v_{\max} - W_i/W (v_{\max} - v_{\min})}. \quad (4)$$

Hence, the total duration of the thief's journey is calculated as follows

$$f(\mathcal{A}, \mathcal{Z}) = \sum_{i=1}^N t_{i,i+1}. \quad (5)$$

After visiting all cities, the total profit the thief obtains is calculated as equal to

$$\sum_{i=1}^N \sum_{k=1}^{|B_{\alpha_i}|} p_{\alpha_i, k} z_{\alpha_i, k} = \sum_{i=1}^N \sum_{k=1}^{|B_i|} p_{i, k} z_{i, k}, \quad (6)$$

where $p_{\alpha_i, k}$ is the profit of the k -th item at the city α_i . Consequently, the second objective of the BI-TTP is mathematically defined as

$$g(\mathcal{A}, \mathcal{Z}) = - \sum_{i=1}^N \sum_{k=1}^{|B_i|} p_{i, k} z_{i, k}, \quad (7)$$

where the negative sign is used to convert the maximization of profit into a minimization objective for consistency with the overall problem formulation. The completed version of BI-TTP is defined as follows

$$\mathcal{A}, \mathcal{Z} = \begin{cases} \text{argmin } f(\mathcal{A}, \mathcal{Z}) \\ \text{argmin } g(\mathcal{A}, \mathcal{Z}) \end{cases} \quad (8a)$$

$$\text{subject to } W_N \leq W. \quad (8b)$$

The two objectives are inherently conflicting: while collecting more items increases the total reward, it also reduces the thief's velocity, thereby leading to longer travel time. This trade-off necessitates a careful balance between maximizing received profit and minimizing travel time. Fig. 1 shows an example, where the thief travels through four cities with different items.

IV. QA-based ε -constraint method

This section proposes a novel approach for solving the BI-TTP by combining QA with the ε -constraint method, termed the QA-based ε -constraint method. We commence by presenting preliminaries on the quantum annealing method, reformulate the problem using binary decision variables, and apply the ε -constraint method to transform this problem into multiple single-objective subproblems.

A. Preliminaries on Quantum Annealing

Quantum annealing (QA) has been widely adopted to solve a broad range of optimization problems. In QA, a quantum processor performs the annealing process on quantum bits (qubits) to minimize an unconstrained Ising model, which is generally formulated as follows:

$$H_{\text{Ising}}(\sigma) = \sum_{i=1}^M h_i \sigma_i + \sum_{i=1}^M \sum_{j=1}^M J_{ij} \sigma_i \sigma_j, \quad (9)$$

where $\sigma_i \in \{-1, 1\}$ represents the spin direction of the i -th qubit, and h_i and J_{ij} denote the qubit bias and coupling strength between qubits, respectively. The corresponding quantum Hamiltonian is given by:

$$H_q(\sigma^x) = \sum_{i=1}^M h_i \sigma_i^x + \sum_{i=1}^M \sum_{j=1}^M J_{ij} \sigma_i^x \sigma_j^x, \quad (10)$$

where σ_i^x denotes the Pauli-X operator acting on the i -th qubit in a Hilbert space of dimension 2^M [42]. To obtain the lowest-energy solution, quantum annealing gradually evolves the system's Hamiltonian through a time-dependent annealing schedule, represented as:

$$H(t) = \left(1 - \frac{t}{T}\right) H_0 + \frac{t}{T} H_q, \forall 0 \leq t \leq T, \quad (11)$$

where $H(t)$ is the Hamiltonian of the quantum system at time t , and T is the total duration of the annealing process, H_0 and H_q denote the initial and final Hamiltonians (the final Hamiltonian is associated with the considered problem), respectively. According to the quantum adiabatic theorem [43], if T is sufficiently large and H_0 does not commute with H_q , the system will remain in its instantaneous ground state throughout the evolution. As a result, the final state of the qubits encodes the global minimum of the original problem. The initial Hamiltonian is typically chosen as $H_0 = -\sum_{i=1}^M \sigma_i^x$ to ensure non-commutativity with H_q and provide a trivial, easily preparable ground state [44].

The QUBO model is a widely adopted framework for representing combinatorial optimization problems as binary quadratic functions. By applying the transformation $x_i = (\sigma_i + 1)/2$, the QUBO formulation corresponding to the Ising model in (9) can be derived as:

$$H_{\text{QUBO}}(\mathbf{x}) = \sum_{i=1}^M Q_{ii}x_i + \sum_{i=1}^M \sum_{j=1}^M Q_{ij}x_i x_j = \mathbf{x}^T \mathbf{Q} \mathbf{x}, \quad (12)$$

where \mathbf{x} is a binary vector with the i -th variable $x_i \in \{0, 1\}$, and $\mathbf{Q} \in \mathbb{R}^{M \times M}$ is the weighted matrix. D-Wave's quantum annealer can solve problems directly when the objective is formulated as a QUBO formulation. However, practical problems naturally involve multiple constraints, which typically take the following form:

$$\underset{\mathbf{x}}{\text{minimize}} \quad H_{\text{cost}}(\mathbf{x}) = \mathbf{x}^T \mathbf{Q} \mathbf{x} \quad (13a)$$

$$\text{subject to } H_c^{(j)}(\mathbf{x}) \leq 0, \forall j = \overline{1, J}. \quad (13b)$$

The common solution to tackle constraints is to introduce a penalty to the constraints [45] and solve the obtained problem,

$$\underset{\mathbf{x}}{\text{minimize}} \quad H_{\text{QUBO}}(\mathbf{x}) = H_{\text{cost}}(\mathbf{x}) - \sum_{j=1}^J \lambda_j H_c^{(j)}(\mathbf{x}). \quad (14)$$

In D-Wave's CQM hybrid solver, penalty coefficients λ_c are automatically calibrated, eliminating the need for manual tuning. This allows users to define linear or quadratic objectives and constraints directly, streamlining the formulation of QUBO models and enabling efficient solution retrieval.

B. Binary Reformulation of the BI-TTP

As QUBO models inherently operate over binary variables, the original problem must be reformulated to express all decision variables in binary form. Therefore, we introduce a binary decision variable $x_{v,i}$, which takes the value 1 if c_v is the i -th city in the tour ($\alpha_i = v$), and 0 otherwise. Since exactly one city must occupy the i -th position in the tour, the following two constraints must be satisfied

$$\sum_{v=1}^N x_{v,i} = 1, \forall i = \overline{1, N}; \quad \sum_{i=1}^N x_{v,i} = 1, \forall v = \overline{1, N}, \quad (15)$$

which dictate that for all $1 \leq v, i, j \leq N$ where $i \neq j$, the condition $x_{v,i} = x_{v,j} = 1$ is strictly prohibited. By ensuring

that no city is visited twice, our binary formulation inherently eliminates the possibility of subtours. Accordingly, the distance from city α_i to α_{i+1} is calculated as follows

$$d_{\alpha_i, \alpha_{i+1}} = \sum_{u=1}^N \sum_{v=1}^N d_{u,v} x_{u,i} x_{v,i+1}. \quad (16)$$

For the given constraints in (15), there exists a unique tuple (u, v, i) such that $x_{u,i} = x_{v,i+1} = 1$, indicating that city c_u is assigned to position i and city c_v to position $i+1$ in the tour. Furthermore, using the binary variables $x_{v,i}$, the knapsack weight after visiting city c_{α_i} , as defined in (1), can be reformulated as:

$$W_i = \sum_{j=1}^i \sum_{t=1}^N \left(x_{t,j} \sum_{k=1}^{|B_t|} z_{t,k} w_{t,k} \right), \quad (17)$$

where $\sum_{k=1}^{|B_t|} z_{t,k} w_{t,k}$ represents the total weight of all items picked at city c_t . To simplify the representation, we define the column vectors $\mathbf{x}_v = [x_{v,1}, \dots, x_{v,i}, \dots, x_{v,N}]^T$ and $\mathbf{z}_i = [z_{i,1}, \dots, z_{i,k}, \dots, z_{i,|B_i|}]^T$, which are then aggregated into the matrices $\mathbf{X} = [\mathbf{x}_1, \dots, \mathbf{x}_v, \dots, \mathbf{x}_N]$ and $\mathbf{Z} = [\mathbf{z}_1, \dots, \mathbf{z}_i, \dots, \mathbf{z}_N]$. The first objective function $f(\mathbf{X}, \mathbf{Z})$ is

$$\begin{aligned} f(\mathbf{X}, \mathbf{Z}) &= \sum_{i=1}^N t_{i,i+1} = \sum_{i=1}^N \frac{\sum_{u=1}^N \sum_{v=1}^N d_{u,v} x_{u,i} x_{v,i+1}}{v_{i,i+1}} \\ &= \sum_{i=1}^N \frac{\sum_{u=1}^N \sum_{v=1}^N d_{u,v} x_{u,i} x_{v,i+1}}{v_{\max} - W_i/W(v_{\max} - v_{\min})} \\ &= \sum_{i=1}^N \frac{W \sum_{u=1}^N \sum_{v=1}^N d_{u,v} x_{u,i} x_{v,i+1}}{W v_{\max} - W_i(v_{\max} - v_{\min})} \end{aligned} \quad (18)$$

Similarly, the second objective $g(\mathbf{X}, \mathbf{Z})$ is computed as

$$g(\mathbf{X}, \mathbf{Z}) = - \sum_{i=1}^N \sum_{t=1}^N \left(x_{t,i} \sum_{k=1}^{|B_t|} z_{t,k} p_{t,k} \right), \quad (19)$$

where $\sum_{k=1}^{|B_t|} z_{t,k} p_{t,k}$ represents the total profit accumulated by the thief after visiting city c_t . The BI-TTP formulation in (8) can now be expressed as:

$$\underset{\mathbf{X}, \mathbf{Z}}{\text{minimize}} \quad f(\mathbf{X}, \mathbf{Z}) = \sum_{i=1}^N \frac{W \sum_{u=1}^N \sum_{v=1}^N d_{u,v} x_{u,i} x_{v,i+1}}{W v_{\max} - W_i(v_{\max} - v_{\min})} \quad (20a)$$

$$g(\mathbf{X}, \mathbf{Z}) = - \sum_{i=1}^N \sum_{t=1}^N \left(x_{t,i} \sum_{k=1}^{|B_t|} z_{t,k} p_{t,k} \right) \quad (20b)$$

$$\text{subject to } \sum_{i=1}^N \sum_{t=1}^N \left(x_{t,i} \sum_{k=1}^{|B_t|} z_{t,k} w_{t,k} \right) \leq W \quad (20c)$$

$$x_{t,i} \in \{0, 1\}, \forall t, i = \overline{1, N} \quad (20d)$$

$$\sum_{v=1}^N x_{v,i} = 1, \forall i = \overline{1, N} \quad (20e)$$

$$\sum_{j=1}^N x_{v,i} = 1, \forall v = \overline{1, N} \quad (20f)$$

$$z_{t,k} \in \{0, 1\}, \forall t = \overline{1, N}, k = \overline{1, |B_t|} \quad (20g)$$

The reformulated problem in (20) is now expressed as a binary optimization problem; however, it still involves the simultaneous optimization of two conflicting objectives, making it challenging to obtain optimal solutions. To address this, the next subsection introduces the use of the ε -constraint method, which transforms the problem into a series of more tractable single-objective subproblems.

Algorithm 1 QA-based ε -constraint method for the BI-TTP

Input: The binary version of the BI-TTP, i.e. problem (20); the number of equal segments S .

Output: The Pareto front of the BI-TTP

- 1: Identify the minimum and the maximum of the second objective (20b) without concerning about the first objective (20a) using QA, denoted as g_{\min} and g_{\max} , respectively.
 - 2: for $0 \leq s < S$ do
 - 3: $\varepsilon_s \leftarrow g_{\min} + s \cdot (g_{\max} - g_{\min})/S$
 - 4: end for
 - 5: for $0 \leq s < S$ do
 - 6: Generate the s -th ε -constraint subproblem by constraining the objective (20b) such that $\varepsilon_s \leq g(\mathbf{X}, \mathbf{Z}) \leq \varepsilon_{s+1}$.
 - 7: Obtain the solution $(\mathbf{X}_s, \mathbf{Z}_s)$ of the s -th subproblem using QA.
 - 8: end for
 - 9: Determine the non-dominated set from identified solutions $(\mathbf{X}_s, \mathbf{Z}_s), \forall 0 \leq s < S$ as the Pareto front.
-

C. Dispensing with ε -constraint method

To solve the binary formulation of the BI-TTP, we propose a novel approach called the QA-based ε -constraint method, which combines QA with the ε -constraint technique. Specifically, we apply the ε -constraint method to transform the bi-objective problem in (20) into a sequence of single-objective subproblems, each of which is solved using quantum annealing. To enable this transformation, the first step involves determining the range of possible knapsack profit values. Let g_{\min} and g_{\max} denote the minimum and maximum achievable profits, respectively, computed without considering the travel time objective. The detailed methodology for identifying these values is given in Subsection V-A.

Given the determined range of knapsack profit, the interval $[g_{\min}, g_{\max}]$ is divided into S segments $[\varepsilon_s, \varepsilon_{s+1}]$, where $g_{\min} = \varepsilon_0 \leq \varepsilon_1 \leq \dots \leq \varepsilon_S = g_{\max}$. In our experiments, we initialize $\varepsilon_s = g_{\min} + s \cdot (g_{\max} - g_{\min})/S, \forall 0 \leq s \leq S$ such that each interval $[\varepsilon_s, \varepsilon_{s+1}]$ covers an equal portion of the value spectrum. For the given knapsack constraint value corresponding to the s -th segment, the associated subproblem is formulated as follows:

$$\text{minimize } f(\mathbf{X}, \mathbf{Z}) = \sum_{i=1}^N \frac{W \sum_{u=1}^N \sum_{v=1}^N d_{u,v} x_{u,i} x_{v,i+1}}{W v_{\max} - W_i (v_{\max} - v_{\min})} \quad (21a)$$

$$\text{subject to } \varepsilon_s \leq g(\mathbf{X}, \mathbf{Z}) \leq \varepsilon_{s+1}, \quad (21b)$$

$$(20c) - (20g),$$

The selection of the number of segments is critical, as if the interval width is too narrow, the feasible region of the corresponding subproblem may become empty, making it unsolvable. Conversely, if the interval is too large, the constraint may become ineffective, reducing its impact on guiding the search. Additionally, each interval

must lie within the range of achievable knapsack profits, i.e., $[g_{\min}, g_{\max}]$, to ensure feasibility. Consequently, in our approach, we divide this interval uniformly into S equal segments, which facilitates uniform coverage of the Pareto front across the objective space. This systematic segmentation also enables effective boundary exploration, leveraging the flexibility of tuning ε , in contrast to the stochastic nature of MOEAs that rely on randomly initialized populations.

The goal in solving the problem in (21) is to minimize the total travel time while satisfying a constraint on the knapsack profit. However, the resulting objective function is expressed as a sum of fractional terms, which poses challenges for direct optimization. To address this, we propose an iterative algorithm that reformulates the objective into an equivalent form suitable for quantum annealing. The detailed transformation and solution procedure are described in Subsection V-B. After solving all subproblems, the final Pareto front is constructed by extracting the set of non-dominated solutions from the union of all obtained results. The overall framework of the proposed approach is summarized in Algorithm 1.

V. Finding solution to the BI-TTP

This section presents the solution procedures for: (i) identifying the upper and lower bounds of the knapsack profit; (ii) minimizing the total travel time under constrained knapsack profit values; and (iii) enhancing the solutions returned by the quantum annealer through a tailored heuristic refinement.

A. Identification of Minimum and Maximum Knapsack Values

The problem of identifying the lower bound of $g(\mathbf{X}, \mathbf{Z})$ is

$$\text{minimize } g(\mathbf{X}, \mathbf{Z}) = - \sum_{i=1}^N \sum_{t=1}^N \left(x_{t,i} \sum_{k=1}^{|B_t|} z_{t,k} p_{t,k} \right) \quad (22a)$$

$$\text{subject to } (20c) - (20g).$$

It is evident that both the objective function and constraints in problem (22) are formulated as linear or quadratic expressions over binary variables, making the problem directly compatible with the D-Wave CQM solver for efficient solution search. In contrast, the maximum value of $g(\mathbf{X}, \mathbf{Z})$ is 0 when the thief does not collect any items along the tour, i.e., $z_{t,k} = 0$ for all $t \in \{1, \dots, N\}$ and $k \in \{1, \dots, |B_t|\}$.

B. The Travel Time Minimization with Constrained Knapsack's Values

The travel time minimization problem, subject to the knapsack value constrained within the segment $[\varepsilon_s, \varepsilon_{s+1}]$,

is rewritten as follows:

$$\begin{aligned} \text{minimize} \quad & f(\mathbf{X}, \mathbf{Z}) = \sum_{i=1}^N \frac{W \sum_{u=1}^N \sum_{v=1}^N d_{u,v} x_{u,i} x_{v,i+1}}{W v_{\max} - W_i(v_{\max} - v_{\min})} \\ \text{subject to} \quad & \varepsilon_s \leq g(\mathbf{X}, \mathbf{Z}) \leq \varepsilon_{s+1}, \\ & (20c) - (20g). \end{aligned} \quad (23)$$

To enable compatibility with quantum annealing, both the objective and the constraints must be reformulated into a QUBO structure. However, the objective function in (23) contains fractional terms, which fall outside the standard quadratic form. To address this challenge, we propose an iterative transformation technique. Specifically, we construct an equivalent formulation of the subproblem (23), grounded in the results established by Lemma 1, as presented below:

Lemma 1. Given the subproblem in (23), we represent it in a more concise form as follows:

$$\begin{aligned} \text{minimize}_{\mathbf{X}, \mathbf{Z}} \quad & \sum_{i=1}^N \frac{A_i(\mathbf{X}, \mathbf{Z})}{B_i(\mathbf{X}, \mathbf{Z})} \\ \text{subject to} \quad & (\mathbf{X}, \mathbf{Z}) \in \mathcal{D} \end{aligned} \quad (24)$$

where $A_i(\mathbf{X}, \mathbf{Z}) = W \sum_{u=1}^N \sum_{v=1}^N d_{u,v} x_{u,i} x_{v,i+1}$ and $B_i(\mathbf{X}, \mathbf{Z}) = W v_{\max} - W_i(v_{\max} - v_{\min}), \forall i = \overline{1, N}$. Here, \mathcal{D} denotes the feasible domain defined by all constraints in problem (23). This problem is equivalent to

$$\begin{aligned} \text{minimize}_{\mathbf{X}, \mathbf{Z}, \mathbf{b}} \quad & \sum_{i=1}^N \frac{A_i(\mathbf{X}, \mathbf{Z})}{b_i} \\ \text{subject to} \quad & B_i(\mathbf{X}, \mathbf{Z}) \geq b_i > 0, \forall i = \overline{1, N}, \\ & (\mathbf{X}, \mathbf{Z}) \in \mathcal{D}, \end{aligned} \quad (25)$$

where $\mathbf{b} = [b_1, b_2, \dots, b_n]^T$.

Proof. See Appendix VIII-A. \square

By applying Lemma 1, the objective is now correctly formulated within the constrained QUBO framework. Therefore, we can now focus on finding optimal solutions of the converted problem (26), which is represented as follows:

$$\begin{aligned} \text{minimize} \quad & f(\mathbf{X}, \mathbf{Z}, \mathbf{b}) = \sum_{i=1}^N \frac{W \sum_{u=1}^N \sum_{v=1}^N d_{u,v} x_{u,i} x_{v,i+1}}{b_i} \\ \text{subject to} \quad & W v_{\max} - W_i(v_{\max} - v_{\min}) \geq b_i, \forall i = \overline{1, N}, \\ & b_i > 0, \forall i = \overline{1, N}, \\ & \varepsilon_s \leq g(\mathbf{X}, \mathbf{Z}) \leq \varepsilon_{s+1}, \\ & (20c) - (20g). \end{aligned} \quad (26)$$

To comprehensively solve the problem in (26), we adopt an iterative approach to alternately optimize the decision variables (\mathbf{X}, \mathbf{Z}) and the auxiliary variable \mathbf{b} .

1) Update solution (\mathbf{X}, \mathbf{Z}) with fixed scalar \mathbf{b} : With the scalar variable \mathbf{b} held constant, this step involves solving

for the variables (\mathbf{X}, \mathbf{Z}) using the CQM solver. Specifically, at the t -th iteration, the problem in (26) becomes

$$\begin{aligned} \text{minimize} \quad & f^{(t)}(\mathbf{X}, \mathbf{Z}, \mathbf{b}) = \sum_{i=1}^N \frac{W \sum_{u=1}^N \sum_{v=1}^N d_{u,v} x_{u,i} x_{v,i+1}}{b_i^{(t-1)}} \\ \text{subject to} \quad & W v_{\max} - W_i(v_{\max} - v_{\min}) \geq b_i^{(t-1)}, \forall i = \overline{1, N}, \\ & \varepsilon_s \leq g(\mathbf{X}, \mathbf{Z}) \leq \varepsilon_{s+1}, \\ & (20c) - (20g), \end{aligned} \quad (27)$$

where $\mathbf{b}^{(t-1)}$ is taken from the previous iteration. The problem conforms to the QUBO model structure and can be efficiently solved using the CQM solver, yielding a low-energy solution $(\mathbf{X}^{\text{QA},(t)}, \mathbf{Z}^{\text{QA},(t)})$ at the t -th iteration.

Note that current quantum processors operate within the noisy intermediate-scale quantum (NISQ) era, where limited coherence times and hardware noise can degrade solution quality [46]. As a result, quantum annealing may yield suboptimal solutions due to noise-induced errors or by becoming trapped in local optima while exploring the feasible space. To mitigate these limitations and improve solution quality, we propose a heuristic post-processing operator, termed Later and Enough Accumulation (LEA).

Observing that selecting items from cities later in the tour keeps the knapsack lighter during earlier moments of the tour, thereby increasing the thief's velocity and reducing overall travel time. Therefore, we propose a selection strategy biased toward accumulating items near the end of the tour. Moreover, the LEA heuristic is designed to guarantee feasibility with respect to the total profit constraint. In particular, the solution $(\mathbf{X}^{\text{LEA}}, \mathbf{Z}^{\text{LEA}})$ is refined so that $g(\mathbf{X}^{\text{LEA}}, \mathbf{Z}^{\text{LEA}})$ is closest to the corresponding threshold ε_s in the s -th subproblem. As a result, this design naturally aligns with the ε -constraint method, while it is not readily compatible with other classical approaches. A detailed description of this operator can be found in Appendix VIII-C.

2) Update auxiliary variable \mathbf{b} based on received (\mathbf{X}, \mathbf{Z}) : Given the enhanced solution $(\mathbf{X}^{(t)}, \mathbf{Z}^{(t)})$, the auxiliary variable $\mathbf{b}^{(t)}$ is updated as follows:

$$b_i = W v_{\max} - W_i(v_{\max} - v_{\min}), \forall i = \overline{1, N}, \quad (28)$$

where this update guarantees the largest reduction of the objective function. The iterative process of updating \mathbf{b} and solving for (\mathbf{X}, \mathbf{Z}) continues until convergence as in Lemma 2.

Lemma 2. Given any initial point $(\mathbf{X}^{(0)}, \mathbf{Z}^{(0)}, \mathbf{b}^{(0)})$ that satisfies the feasibility conditions of problem (26), the iterative procedure, solving the subproblem in (27) to update (\mathbf{X}, \mathbf{Z}) and then updating \mathbf{b} using (28), progressively narrows the search space and guarantees convergence.

Proof. See Appendix VIII-B. \square

Based on the above formulation, the complete framework for solving problem (26) is outlined in Algorithm 2. Initially, the auxiliary variable \mathbf{b} is set to $\mathbf{1}^T$, which provides a small and positive starting point preserving

Algorithm 2 Iterative Approach for problem (26)

Input: The distance from two arbitrary cities u and v : $d_{u,v}$ with $u, v = \overline{1, N}$; the bag's capacity W ; the maximum and minimum velocity of the thief: v_{\max} and v_{\min} ; the profit of k -th item at city t : $p_{t,k}$ with $t = \overline{1, N}$, $k = \overline{1, |\mathcal{B}_t|}$; two endpoints of segment $\varepsilon_s, \varepsilon_{s+1}$ and auxiliary variable \mathbf{b} ; the maximum number of iterations T .

Output: The traveling strategy \mathbf{X} and the picking plan \mathbf{Z}

- 1: Set the iteration index $t \leftarrow 0$, the auxiliary vector $\mathbf{b}^{(t)} \leftarrow \mathbf{1}_N^T$, where $\mathbf{1}_N$ is a vector having N elements equal to 1.
 - 2: while $t < T$ do
 - 3: $t \leftarrow t + 1$
 - 4: Use QA to identify solution $(\mathbf{X}^{\text{QA},(t)}, \mathbf{Z}^{\text{QA},(t)})$ of problem (26).
 - 5: $(\mathbf{X}^{(t)}, \mathbf{Z}^{(t)}) \leftarrow \text{LEA}(\mathbf{X}^{\text{QA},(t)}, \mathbf{Z}^{\text{QA},(t)})$
 - 6: Obtain $\mathbf{b}^{(t)}$ by (28)
 - 7: if $f(\mathbf{X}^{(t)}, \mathbf{Z}^{(t)}, \mathbf{b}^{(t)}) < f(\mathbf{X}^{(t-1)}, \mathbf{Z}^{(t-1)}, \mathbf{b}^{(t-1)})$ then
 - 8: break
 - 9: end if
 - 10: end while
 - 11: return $\mathbf{X}_s = \mathbf{X}^{(t-1)}, \mathbf{Z}_s = \mathbf{Z}^{(t-1)}$
-

the feasibility of problem (26). During each iteration, the decision variables \mathbf{X} and \mathbf{Z} , along with \mathbf{b} , are updated in an alternating fashion. Specifically, a candidate solution (\mathbf{X}, \mathbf{Z}) is first obtained using the CQM solver. This solution is then refined via the proposed LEA heuristic to improve quality. Subsequently, with (\mathbf{X}, \mathbf{Z}) fixed, the auxiliary variable \mathbf{b} is updated using the rule defined in equation (28). The process repeats until either the objective value fails to improve or a predefined iteration limit is reached.

C. Variable Utilization and Computational Complexity

Since D-Wave hardware restricts the number of variables to at most 500000, it is crucial to carefully analyze variables consumption when encoding the BI-TTP into a QUBO formulation. For the binary tour variable $x_{v,i}$ with $1 \leq v, i \leq N$, we have utilized $N \times N = N^2$ variables. Similarly, for the picking variable $z_{i,k}$ with $1 \leq i \leq N, 1 \leq k \leq |\mathcal{B}_i|$, the encoding requires $N \times \max_{1 \leq i \leq N} |\mathcal{B}_i|$ variables. Therefore, the total number of variables used in our encoding is $N \times (N + \max_{1 \leq i \leq N} |\mathcal{B}_i|)$.

Regarding the time complexity, for a problem involving K binary variables, the theoretical time complexity of quantum annealing (QA) is $\mathcal{O}(e^{\sqrt{K}})$, as established in [47]. In our formulation, the traveling strategy \mathbf{X} and the item selection plan \mathbf{Z} require $\mathcal{O}(N^2)$ and $\mathcal{O}(NM)$ binary variables, respectively, where N is the number of cities and M is the total number of items. Therefore, the time complexity for computing the minimum and maximum bounds of the second objective is $\mathcal{O}(e^{\sqrt{N^2+NM}})$. Given that the range of the second objective is divided into S equal segments, S subproblems must be solved. For

TABLE I: Information of considered instances

Instances	n	m	W	Knapsack Type
ch150_n149_bsc	150	149	12310	bsc
ch150_n149_unc	150	149	6860	unc
ch150_n149_usw	150	149	13608	usw
a280_n279_bsc	280	279	25936	bsc
a280_n279_unc	280	279	12718	unc
a280_n279_usw	280	279	25478	usw

each subproblem, each iteration involves one QA call and one application of the LEA heuristic, with complexities of $\mathcal{O}(e^{\sqrt{N^2+NM}})$ and $\mathcal{O}(M^2)$, respectively. After obtaining S solutions from the subproblems, identifying the non-dominated set to construct the Pareto front incurs a computational cost of $\mathcal{O}(S \log S)$, as discussed in [48]. Therefore, the overall computational complexity of the proposed algorithm is $\mathcal{O}(STe^{\sqrt{n^2+nm}} + STm^2 + S \log S)$, where T denotes the number of iterations required for convergence.

It is important to note that the aforementioned time complexity is derived under the assumption of classical simulation of quantum annealing. In contrast, our proposed approach utilizes D-Wave's Leap Service, which employs a quantum-classical hybrid CQM solver that integrates advanced classical heuristics with quantum processing capabilities. By exploiting quantum phenomena such as superposition and entanglement, the QPU can simultaneously explore a vast portion of the solution space, thereby enabling near-optimal solutions to be found in significantly reduced time. A comprehensive performance evaluation is provided in Section VI.

VI. Numerical Results

This section presents experimental results validating the effectiveness of the proposed approach using diverse benchmark instances to ensure generality across various settings.

A. Experimental Setup

Environment. All experiments were conducted on Kaggle using an Intel(R) Xeon(R) CPU (4 cores, 2.20 GHz) with 30 GB RAM. The implementation environment includes Python 3.10, Dimod 0.12, D-Wave System 1.32, and Pymoo 0.6. All experiments were conducted on the D-Wave Advantage2 Quantum Processing Units (QPUs), which support up to 4,400 qubits and 40,000 couplers. The Advantage2 QPU employs the Zephyr topology, in which each qubit is connected to 16 orthogonal neighboring qubits via internal couplers, along with 2 external couplers and 2 odd couplers that link it to similarly oriented qubits. Furthermore, the QUBO formulation is implemented using D-Wave's Constrained Quadratic Model (CQM) framework and solved through the Leap Service's hybrid quantum-classical CQM solver. Consequently, the reported runtime corresponds to the total time CQM solver spent working on each problem, encompassing QPU access time and classical postprocessing time.

Datasets. We employ the instances `ch150_n149` and `a280_n279` from [24], which differ in the number of cities and items. Notably, the `a280_n279_bcs` instance has been widely adopted in BI-TTP competitions at EMO-2019³, GECCO-2019⁴, and GECCO-2024⁵. Detailed characteristics of the test cases are provided in Table I, where N , M , and W denote the number of cities, items, and knapsack capacity, respectively. Item weights follow three standard distributions: bounded strongly correlated (`bsc`), uncorrelated (`unc`), and uncorrelated with similar weights (`usw`). For main results, the number of ε -segments S is set to 10.

Baselines. For comparison, we evaluate the performance of our approach against state-of-the-art classical MOEAs widely used for solving bi-objective optimization problems: NSGA-II [26] and U-NSGA-III [27]. Both NSGA-II and U-NSGA-III extend the genetic algorithm (GA) framework [49] by employing non-dominated sorting to address multi-objective optimization, focusing on approximating the Pareto front rather than optimizing a single objective. While retaining the core GA operations, crossover and mutation, they differ in selection mechanisms: NSGA-II employs non-dominated sorting and crowding distance for forming the next population, whereas U-NSGA-III utilizes a set of reference directions to encourage uniform Pareto front distribution. We further consider the MOEA/D algorithm [25], an alternative multi-objective evolutionary algorithm that employs a distinct decomposition strategy to transform a multi-objective problem into multiple single-objective subproblems. We implement three algorithms using the Pymoo framework [50], which streamlines the development of evolutionary optimization methods. Following the configuration in [34], we set the population size to 500, the crossover rate to 0.8, and the mutation rate to 0.1. We run these baselines for 10000 iterations on the `a280_n279` instance and 4000 iterations on `ch150_n149`.

Metrics. We utilize Hypervolume (HV) and running time to evaluate our method for different methods. HV is a widely adopted metric for evaluating the quality of Pareto fronts in multi-objective optimization, as it reflects how close the solutions are to the true Pareto front and the diversity of the non-dominated solutions obtained [51]. A crucial element in HV calculation is the reference point. Following the protocols established in GECCO-2019 and EMO-2019, the reference point is chosen based on all outcomes from compared algorithms. Particularly, we normalize all considered points via min-max scaling and use the reference point $[1, 1]^T$, which represents the worst scaled outcome for each objective. The HV is hence calculated as the overall area dominated by all points in the Pareto front with respect to the chosen reference point. In terms of computational time, that of the classical baseline algorithms are recorded end-to-end, while the runtime of the proposed hybrid approach is obtained by

aggregating the execution times returned by the D-Wave framework.

B. Comparison with State-of-the-art methods

Fig. 2 illustrates the evolution of the hypervolume (HV) for different methods. Since our quantum-based method generates a complete, high-quality Pareto front in a single run, we incrementally merge the evolving solutions from NSGA-II and U-NSGA-III with our fixed Pareto front at each iteration to enable a fair comparison. As a result, Fig. 2 exhibits that the HV curve of our method presents a slight decreasing trend, not due to solution degradation, but due to the integration of intermediate solutions from the evolving fronts of the evolutionary algorithms. Across all three subfigures, the hypervolume (HV) of our quantum-based method consistently exceeds 0.7, indicating a well-distributed Pareto front that effectively dominates a substantial portion of the feasible region, which is widely regarded as a hallmark of high-quality solutions in multi-objective optimization [51]. Notably, in subfigure (2a), U-NSGA-III requires after 10000 iterations cannot match the HV achieved by our method in a single quantum-assisted run. Meanwhile, although U-NSGA-III gradually converges toward comparable HV levels, it remains less stable in reaching competitive front quality, as illustrated in subfigures (2b) and (2c). By contrast, MOEA/D struggles to achieve comparable solution quality on all benchmark instances. This limitation arises because the MOEA/D framework decomposes a multi-objective problem into multiple subproblems using scalar objective weights, which makes it difficult to capture the complex interactions between objectives in the BI-TTP.

Fig. 3 illustrates the Pareto fronts generated by different methods for the `a280_n279` instance. The privileged advantage of the proposed QA-based ε -constraint method is its systematic strategy for covering the full range of the second objective by dividing it into uniformly spaced intervals. This structured exploration generates well-distributed solutions along the axis of the second objective, enabling the resulting Pareto front to span a wide spectrum of trade-offs. In contrast, NSGA-II and U-NSGA-III rely heavily on the initial population and their evolutionary mechanisms, limiting the capability of consistently exploring the entire objective space. As shown in Fig. 3, their performance varies significantly across different instances. For example, all algorithms perform relatively well on the `a280_n279_usw` instance, likely due to the uniformity in item weights, which simplifies the trade-off between travel time and item selection. However, on the more complex `a280_n279_bcs` instance, where item weights are strongly correlated with profits and require more sophisticated decision-making, both NSGA-II and U-NSGA-III fail to cover the lower end of the second objective spectrum, leaving solutions with values below $-30,000$ undominated. Similarly, for the `a280_n279_unc` instance, the Pareto fronts obtained by NSGA-II and U-NSGA-III are concentrated around the central region of

³<https://www.egr.msu.edu/coinlab/blankjul/emo19-thief/>

⁴<https://www.egr.msu.edu/coinlab/blankjul/gecco19-thief/>

⁵<https://sites.google.com/view/ttp-gecco2024/>

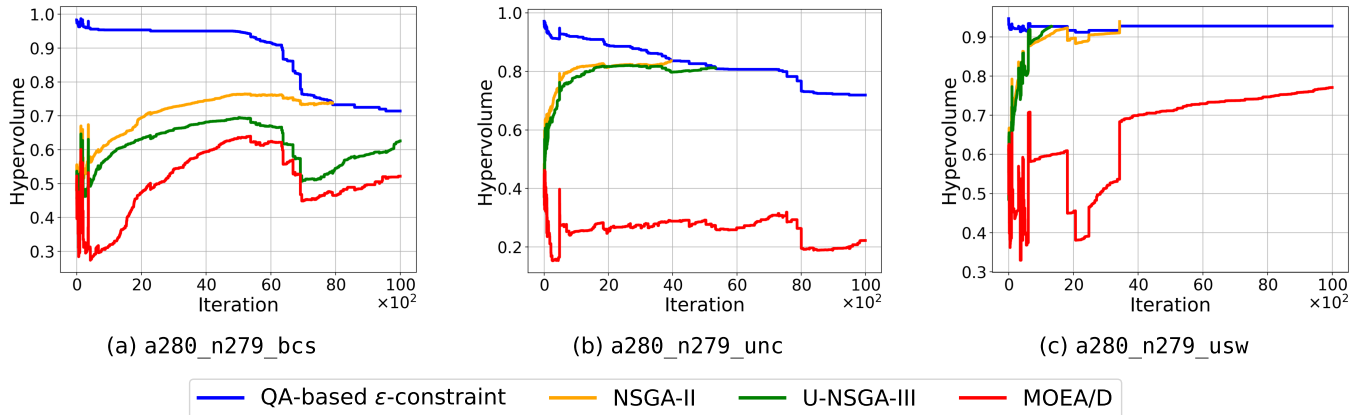


Fig. 2: The HV of QA-based ε -constraint method, NSGA-II, U-NSGA-III, and MOEA/D at each iteration corresponding to the instance a280_n279. Our method produces a complete and high-quality Pareto front via Quantum Annealing, after which the evolving solution sets of NSGA-II, U-NSGA-III, and MOEA/D are incrementally compared at each iteration.

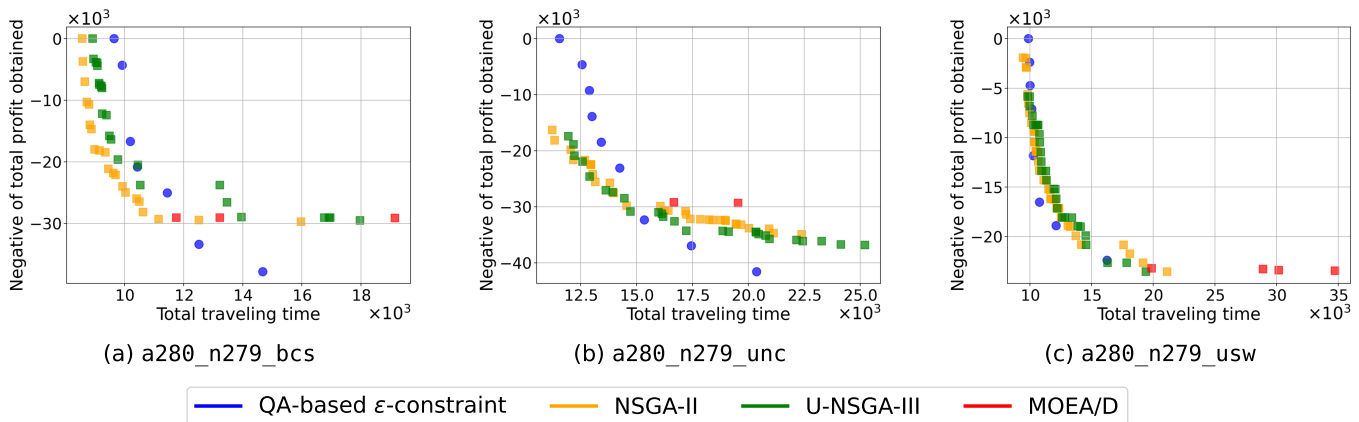


Fig. 3: Comparison of Pareto fronts produced by NSGA-II, U-NSGA-III, MOEA/D, and the QA-based ε -constraint method for the instance a280_n279. Our approach consistently yields well-distributed solutions along the second objective across all instances, while NSGA-II and U-NSGA-III, show considerable variation across instances as a result of their reliance on the initialization process. Furthermore, MOEA/D fails to adequately explore the feasible region and frequently collapses to nearly identical values on the second objective.

	ch150_n149_bcs	ch150_n149_unc	ch150_n149_usw	a280_n279_bcs	a280_n279_unc	a280_n279_usw
Total QPU time	1.2938 \pm 0.0690	1.2993 \pm 0.1280	1.3336 \pm 0.0054	1.4070 \pm 0.0395	1.3991 \pm 0.0325	1.3362 \pm 0.0010
MOEA/D	9678 \pm 197	10079 \pm 657	9718 \pm 273	38170 \pm 884	41614 \pm 265	40672 \pm 967
NSGA-II	5431 \pm 239 (7.5 \times)	1708 \pm 498 (2.1 \times)	917 \pm 57 (1.3 \times)	33771 \pm 4018 (8.1 \times)	16907 \pm 3191 (4.0 \times)	13229 \pm 2553 (3.3 \times)
U-NSGA-III	8712 \pm 135	1365 \pm 85 (1.9 \times)	966 \pm 155 (1.3 \times)	38977 \pm 732	17900 \pm 4583 (4.2 \times)	8484 \pm 2714 (2.1 \times)
Ours (without LEA)	724 \pm 8	719 \pm 5	726 \pm 5	4144 \pm 42	4203 \pm 10	3998 \pm 142
Ours (with LEA)	727 \pm 9	723 \pm 5	728 \pm 5	4161 \pm 41	4227 \pm 11	4006 \pm 142

TABLE II: Comparison of computational time between the proposed method and three baseline algorithms, namely MOEA/D, NSGA-II, and U-NSGA-III. The row labeled “Total QPU time” reports the quantum processing unit (QPU) usage time of our approach, whereas all remaining entries correspond to the overall runtime. For the baseline methods, runtime is measured either at the iteration where their solutions are compared with those produced by our approach or upon algorithm termination. The rows “Ours (without LEA)” and “Ours (with LEA)” denote the proposed method evaluated without and with the LEA heuristic, respectively. Bolded values indicate that the corresponding algorithm reached its termination criterion. Values shown in parentheses ($a\times$) represent the computational overhead relative to our method. All reported results are averaged over three independent runs to ensure fair comparison.

the feasible space, failing to capture extreme trade-offs near the lower and upper bounds of the second objective.

Table II reports the runtime statistics (in seconds) for all compared algorithms across various benchmark instances. For our proposed QA-based ε -constraint method, we separately list the total quantum processing unit (QPU) time and the overall execution time, which includes data preprocessing, classical optimization steps prior to QPU invocation, and the application of the LEA heuristic for post-solution refinement. The reported results show that our approach consistently finds high-quality Pareto fronts faster than classical methods across all BI-TTP instances. Notably, the total runtime and QPU access time for each instance are almost equal, as both are primarily governed by the CQM solver, depending on problem size, input variables, and constraint complexity. In contrast, the classical methods exhibit high runtime variability, as their performance is highly sensitive to the choice of initialization.

Interestingly, in the strongly correlated bounded item distribution setting, U-NSGA-III is likewise unable to match the solution quality achieved by our approach. More importantly, our method also achieves solutions up to 8.1 times faster than NSGA-II on the a280_n279_bcs benchmark, which is recognized as one of the standard benchmarks for algorithm comparison in the BI-TTP competitions at EMO-2019⁶, GECCO-2019⁷, and GECCO-2024⁸. Furthermore, the runtime advantage over classical baselines becomes increasingly pronounced for the a280_n279 instance compared to ch150_n149, as the computational overhead relative to our proposed method consistently increases across all instances, thereby underscoring the superior scalability of the proposed approach on larger problem instances. Consequently, QA is able to produce high-quality solutions that state-of-the-art classical baselines may fail to obtain, highlighting the effectiveness of quantum hardware in exploiting the overall feasible search space within a limited time budget. Finally, the runtime overhead associated with LEA at all benchmarks constitutes only up to 0.5% of the total execution time of the proposed approach and is therefore negligible.

C. Ablation Study

This section focuses on analyzing the efficacy of the proposed QA-based ε -constraint method. We first demonstrate the advantages of the ε -constraint utilization in our hybrid framework over the weighted-sum method. Next, we examine the contribution of the LEA heuristic to solution improvement. Finally, we analyze the quality of the obtained solutions under different values of the parameter S and varying ε -levels. All experiments are performed on the instance a280_n279.

To demonstrate the advantage of explicitly controlling the second objective via the ε -constraint framework, we

	a280_n279_bcs	a280_n279_unc	a280_n279_usw
Weighted-sum (w/o LEA)	0.64 ± 0.02	0.54 ± 0.22	0.55 ± 0.01
ε -constraint (w/o LEA)	0.71 ± 0.02	0.73 ± 0.03	0.75 ± 0.06
ε -constraint (with LEA)	0.89 ± 0.03	0.89 ± 0.04	0.87 ± 0.02

TABLE III: Comparison of hypervolume (HV) obtained by different approaches for addressing the bi-objective BI-TTP. The “Weighted-sum (w/o LEA)” row represents the scalarized formulation of the two objectives in problem (20). The “ ε -constraint” rows correspond to our proposed framework, evaluated with and without the LEA heuristic.

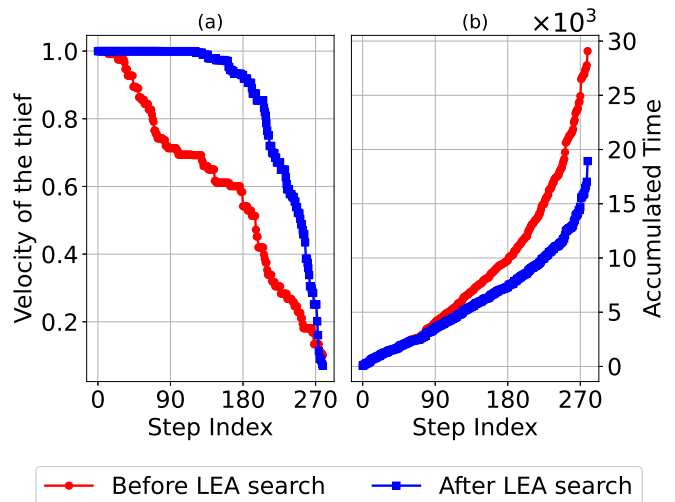


Fig. 4: The change in solution before and after applying LEA search

compare our method against a weighted-sum approach. In particular, the objectives in problem (20) are aggregated into a single scalar objective given by $\alpha \cdot f(\mathbf{X}, \mathbf{Z}) + (1 - \alpha) \cdot g(\mathbf{X}, \mathbf{Z})$. To ensure a fair comparison with S subproblems, the weight parameter is chosen as $\alpha_k = k/(S - 1)$ for $k = 0, \dots, S - 1$. Moreover, as the LEA heuristic is tailored specifically to the ε -constraint method and is not applicable to the weighted-sum formulation, it is excluded from this experiment. As shown in Table III, the proposed ε -constraint framework achieves up to 35% higher solution quality than the weighted-sum approach under the same number of runs. This performance gap arises because the weighted-sum formulation lacks explicit control over the second objective. Notably, the variance observed for the instance a280_n279_unc is relatively large, as the item weights are independently distributed, further highlighting the importance of explicitly controlling one objective when addressing complicated multi-objective problems.

We now further examine the impact of the proposed LEA heuristic on the overall performance of our approach. As reported in Table III, despite its negligible computational overhead, LEA contributes significantly to improving solution quality at all benchmarks. To provide a clearer

⁶<https://www.egr.msu.edu/coinlab/blankjul/emo19-thief/>

⁷<https://www.egr.msu.edu/coinlab/blankjul/gecco19-thief/>

⁸<https://sites.google.com/view/ttp-gecco2024/>

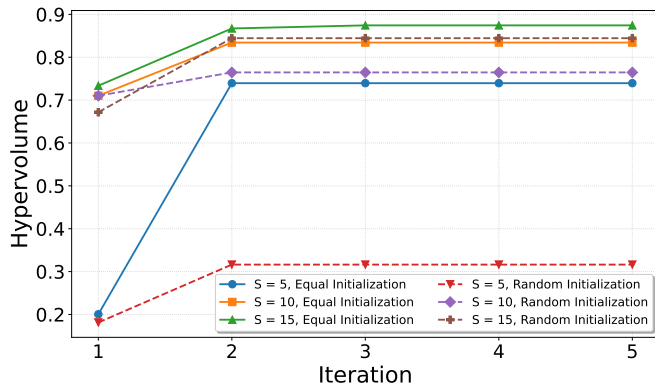


Fig. 5: Sensitivity analysis of the QA-based ε -constraint method with respect to the number of segments S and the initialization of the ε levels.

illustration, Fig. 4 presents a comparison of the thief’s velocity and total travel time for a representative Pareto-optimal solution from the a280_n279_bcs instance, specifically the solution with the lowest travel time. As shown in subfigure (4a), the thief initially moves at maximum velocity, but without LEA (red line), the velocity rapidly decreases due to early item collection. In contrast, with LEA (blue line), velocity remains higher and more stable after the first third of the tour. This results in significantly reduced travel time, as shown in subfigure (4b), where the total duration drops from approximately 29,000 seconds to 18,000 seconds, an improvement of nearly 40%.

We conduct a detailed ablation study to evaluate the effects of the number of segments S and the initialization strategy for the ε levels $\varepsilon_0, \varepsilon_1, \dots, \varepsilon_S$. All experiments are performed on the most challenging benchmark instance, a280_n279_bcs. We vary the number of segments with $S \in \{5, 10, 15\}$. In addition, we compare different initialization strategies for the ε -levels. Specifically, in contrast to the equal initialization strategy, where $\varepsilon_s = g_{\min} + \frac{s}{S}(g_{\max} - g_{\min})$, we also consider a random initialization scheme defined as $\varepsilon_s = g_{\min} + t_s(g_{\max} - g_{\min})$, where $t_0 \leq t_1 \leq \dots \leq t_S$ are randomly sampled from a uniform distribution over $[0, 1]$. As illustrated in Fig. 5, the solution quality exhibits a slight improvement when $S = 15$ under the equal initialization strategy, while all approaches converge by the second iteration. This behavior stems from the effectiveness of QA in producing high-quality near-optimal solutions with a single execution. Furthermore, when the number of segments is set to $S = 10$, the resulting HV is significantly higher than that obtained with $S = 5$. In contrast, increasing the number of segments to $S = 15$ yields only marginal additional improvement. Therefore, $S = 10$ provides a favorable trade-off between computational efficiency and solution quality. Furthermore, across all values of S , the equal initialization strategy consistently outperforms the randomized initialization. This advantage arises because equal initialization enables a more uniform exploration of the feasible space and maintains appropriate spacing along

the second objective. In contrast, random initialization often generates solutions that are either overly clustered or widely dispersed, resulting in less effective coverage of the non-dominated region.

VII. Conclusion

In this paper, we addressed the Bi-Objective Traveling Thief Problem (BI-TTP), which jointly optimizes two conflicting objectives: minimizing travel time and maximizing knapsack profit. To solve this challenging problem, we proposed a novel hybrid quantum-classical framework that combines the ε -constraint method with quantum annealing (QA). By first determining the feasible range of knapsack profits using QA, we systematically partitioned this range into uniform ε intervals, each defining a subproblem with a constrained second objective. These subproblems were reformulated into QUBO models through an auxiliary-variable transformation, enabling direct solution via the D-Wave hybrid CQM solver. Furthermore, we introduced a domain-specific heuristic, called LEA search, to refine QA-generated solutions. Extensive numerical experiments on benchmark instances demonstrated that our method efficiently approximates the Pareto front and significantly reduces computation time compared to classical multi-objective evolutionary algorithms. Looking forward, with advances in quantum hardware, particularly in the number of qubits and QPU reliability, the proposed framework holds promise for solving large-scale, bi-objective combinatorial problems more efficiently.

VIII. Appendix

A. Proof of Lemma 1

Proof. To prove the equivalence between problems (24) and (25), we show that they share the same optimal solution and optimal value. Let $(\mathbf{X}^*, \mathbf{Z}^*, \mathbf{b}^*)$ be the global optimal solution for the problem in (25). Since $0 < b_j^* \leq B_j(\mathbf{X}^*, \mathbf{Z}^*)$, we have

$$\sum_{j=1}^N \frac{A_j(\mathbf{X}^*, \mathbf{Z}^*)}{b_j^*} \geq \sum_{j=1}^N \frac{A_j(\mathbf{X}^*, \mathbf{Z}^*)}{B_j(\mathbf{X}^*, \mathbf{Z}^*)}. \quad (29)$$

On the other hand, let $\tilde{b}_j = B_j(\mathbf{X}^*, \mathbf{Z}^*)$, $\forall j = \overline{1, N}$. Then $(\mathbf{X}^*, \mathbf{Z}^*, \tilde{\mathbf{b}})$ is a feasible solution of problem (25). Since $(\mathbf{X}^*, \mathbf{Z}^*, \mathbf{b}^*)$ is the global optimal solution of problem (25), it follows that

$$\sum_{j=1}^N \frac{A_j(\mathbf{X}^*, \mathbf{Z}^*)}{b_j^*} \leq \sum_{j=1}^N \frac{A_j(\mathbf{X}^*, \mathbf{Z}^*)}{\tilde{b}_j} = \sum_{j=1}^N \frac{A_j(\mathbf{X}^*, \mathbf{Z}^*)}{B_j(\mathbf{X}^*, \mathbf{Z}^*)} \quad (30)$$

From (29) and (30), we deduce that

$$\sum_{j=1}^N \frac{A_j(\mathbf{X}^*, \mathbf{Z}^*)}{b_j^*} = \sum_{j=1}^N \frac{A_j(\mathbf{X}^*, \mathbf{Z}^*)}{B_j(\mathbf{X}^*, \mathbf{Z}^*)} \quad (31)$$

This result implies that $b_j^* = B_j(\mathbf{X}^*, \mathbf{Z}^*)$, $\forall j = \overline{1, N}$. For any $(\mathbf{X}^0, \mathbf{Z}^0) \in \mathcal{D}$, let $b_j^0 = B_j(\mathbf{X}^0, \mathbf{Z}^0)$, $\forall j = \overline{1, N}$. Then

$(\mathbf{X}^0, \mathbf{Z}^0, \mathbf{b}^0)$ is a feasible solution of problem (25), leading to

$$\begin{aligned} & \sum_{j=1}^N \frac{A_j(\mathbf{X}^*, \mathbf{Z}^*)}{B_j(\mathbf{X}^*, \mathbf{Z}^*)} \\ &= \sum_{j=1}^N \frac{A_j(\mathbf{X}^*, \mathbf{Z}^*)}{b_j^*} \leq \sum_{j=1}^N \frac{A_j(\mathbf{X}^0, \mathbf{Z}^0)}{b_j^0} = \sum_{j=1}^N \frac{A_j(\mathbf{X}^0, \mathbf{Z}^0)}{B_j(\mathbf{X}^0, \mathbf{Z}^0)}. \end{aligned} \quad (32)$$

Therefore, $(\mathbf{X}^*, \mathbf{Z}^*)$ is also the global optimal solution of problem (24), and both problems (24) and (25) attain the same minimum objective value. The converse follows by similar reasoning, thereby completing the proof. \square

B. Proof of Lemma 2

Proof. Suppose $(\mathbf{X}^{(t)}, \mathbf{Z}^{(t)}, \mathbf{b}^{(t)})$ is the solution identified at the t -th iteration. At the $(t+1)$ -th iteration, each element of the vector $\mathbf{b}^{(t+1)}$ is updated as

$$b_i^{(t+1)} = Wv_{\max} - W_i^{(t)}(v_{\max} - v_{\min}), \forall i = \overline{1, N}, \quad (33)$$

The constraint at the t -th iteration indicates that $b_i^{(t+1)} \geq b_i^{(t)}$, while at the $t+1$ -th iteration, it becomes

$$Wv_{\max} - W_i^{(t+1)}(v_{\max} - v_{\min}) \geq b_i^{(t+1)}, \forall i = \overline{1, N}. \quad (34)$$

From equations (33) and (34), it follows that $W_i^{(t)} \geq W_i^{(t+1)}$ for all t . Consequently, we have

$$\Theta_{t+1} = \Theta_t \bigcap_{i=1}^N \left\{ W_i^{(t+1)}(\mathbf{X}^{(t+1)}, \mathbf{Z}^{(t+1)}) \leq W_i^{(t)} \right\} \subseteq \Theta_t, \quad (35)$$

where Θ_t denotes the feasible region at iteration t . Therefore, the update guaranties a monotonic reduction in the search space. Since the overall feasible space is finite, the iterative procedure always converges. \square

C. Detail description of our proposed Later and Enough Accumulation heuristic search

The proposed LEA method operates in two phases: the first phase shifts the item selection toward the later cities in the tour, and the second phase iteratively reduces the total weight of the selected items while ensuring compliance with the knapsack capacity constraint. To facilitate this process, the picking plan $\mathbf{Z}^{\text{QA},(t)}$ is flattened into a single vector as follows:

$$\mathbf{Z}^{\text{LEA}} = \left[\mathbf{z}_{\alpha_1}^{\text{QA},(t)}; \mathbf{z}_{\alpha_2}^{\text{QA},(t)}; \dots; \mathbf{z}_{\alpha_N}^{\text{QA},(t)} \right]. \quad (36)$$

Here, we recall that c_{α_i} denotes the i -th city visited in the tour. In the first phase, the proposed LEA algorithm iteratively loops through all elements of the picking vector \mathbf{Z}^{LEA} . At the p -th iteration, if $[\mathbf{Z}^{\text{LEA}}]_p = 1$, the algorithm searches for an index $q > p$ where $[\mathbf{Z}^{\text{LEA}}]_q = 0$. If replacing $[\mathbf{Z}^{\text{LEA}}]_p$ with 0 and $[\mathbf{Z}^{\text{LEA}}]_q$ with 1 maintains the feasibility and leads to a reduction in total travel time, the change is accepted. This selection strategy encourages the thief to prioritize item collection near the end of the tour, while ensuring that the total number of selected items

Algorithm 3 Later and Enough Accumulation (LEA)

Input: the traveling strategy $\mathbf{X} = \mathbf{X}^{\text{QA},(t)}$, the corresponding picking plan $\mathbf{Z} = \mathbf{Z}^{\text{QA},(t)}$

Output: New picking plan \mathbf{Z}^{LEA}

```

1:  $\mathbf{Z}^{\text{LEA}} \leftarrow \mathbf{Z}$ 
2: for  $1 \leq p < M$  do ▷ Phase 1
3:   for  $p+1 \leq q \leq M$  do
4:     if  $([\mathbf{Z}^{\text{LEA}}]_p, [\mathbf{Z}^{\text{LEA}}]_q) = (1, 0)$  then
5:        $\mathbf{Z}^{\text{swap}} \leftarrow \mathbf{Z}^{\text{LEA}}, \text{Swap}([\mathbf{Z}^{\text{swap}}]_p, [\mathbf{Z}^{\text{swap}}]_q)$ 
6:       if  $f(\mathbf{X}, \mathbf{Z}^{\text{swap}}) < f(\mathbf{X}, \mathbf{Z}^{\text{LEA}})$  &  $(\mathbf{X}, \mathbf{Z}^{\text{swap}}) \in \mathcal{D}$ 
       then
7:          $\mathbf{Z}^{\text{LEA}} \leftarrow \mathbf{Z}^{\text{swap}}$ 
8:       end if
9:     end if
10:  end for
11: end for
12: for  $1 \leq p \leq M$  do ▷ Phase 2
13:   if  $[\mathbf{Z}^{\text{LEA}}]_p = 1$  then
14:      $\mathbf{Z}^{\text{temp}} \leftarrow \mathbf{Z}^{\text{LEA}}, [\mathbf{Z}^{\text{temp}}]_p \leftarrow 0$ 
15:     if  $(\mathbf{X}, \mathbf{Z}^{\text{temp}}) \in \mathcal{D}$  then
16:        $\mathbf{Z}^{\text{LEA}} \leftarrow \mathbf{Z}^{\text{temp}}$ 
17:     end if
18:   end if
19: end for
20: return  $\mathbf{Z}^{(t)} = \mathbf{Z}^{\text{LEA}}$  and  $\mathbf{X}^{(t)} = \mathbf{X}^{\text{QA},(t)}$ .
```

remains unchanged. In the second phase, the heuristic iterates through all elements of \mathbf{Z}^{LEA} obtained from the first phase. For each index p where $[\mathbf{Z}^{\text{LEA}}]_p = 1$, the item is deselected (i.e., $[\mathbf{Z}^{\text{LEA}}]_p = 0$) if the solution still satisfies the knapsack constraint and maintains Pareto optimality. The detailed process is in Algorithm 3.

References

- [1] J. D. Malcolm, A. Roth, M. Radic, P. Martin-Ramiro, J. Oillarburu, B. Aizpurua, R. Orús, and S. Mugel, "Multi-disk clutch optimization using quantum annealing," *IEEE Transactions on Quantum Engineering*, 2024.
- [2] C. Chauhan, R. Gupta, and K. Pathak, "Survey of methods of solving tsp along with its implementation using dynamic programming approach," *International journal of computer applications*, vol. 52, no. 4, 2012.
- [3] J. Kusyik, S. M. Saeed, and M. U. Uyar, "Survey on quantum circuit compilation for noisy intermediate-scale quantum computers: Artificial intelligence to heuristics," *IEEE Transactions on Quantum Engineering*, vol. 2, pp. 1–16, 2021.
- [4] T. Stollenwerk, S. Hadfield, and Z. Wang, "Toward quantum gate-model heuristics for real-world planning problems," *IEEE Transactions on Quantum Engineering*, vol. 1, pp. 1–16, 2020.
- [5] T. Van Chien, B. T. Duc, H. V. D. Luong, H. T. T. Binh, H. Q. Ngo, and S. Chatzinotas, "Active and Passive Beamforming Designs for SER Minimization in RIS-Assisted MIMO Systems," *IEEE Transactions on Wireless Communications*, 2024.
- [6] N. X. Tung, T. Van Chien, D. T. Hoang, and W. J. Hwang, "Jointly Optimizing Power Allocation and Device Association for Robust IoT Networks under Infeasible Circumstances," *IEEE Transactions on Network and Service Management*, 2024.
- [7] J. Wang, B. Cen, S. Gao, Z. Zhang, and Y. Zhou, "Cooperative evolutionary framework with focused search for many-objective optimization," *IEEE Transactions on Emerging Topics in Computational Intelligence*, vol. 4, no. 3, pp. 398–412, 2018.

- [8] R. T. Marler and J. S. Arora, "The weighted sum method for multi-objective optimization: new insights," *Structural and multidisciplinary optimization*, vol. 41, pp. 853–862, 2010.
- [9] J. Aghaei, N. Amjadi, and H. A. Shayanfar, "Multi-objective electricity market clearing considering dynamic security by lexicographic optimization and augmented epsilon constraint method," *Applied Soft Computing*, vol. 11, no. 4, pp. 3846–3858, 2011.
- [10] I. Das and J. E. Dennis, "A closer look at drawbacks of minimizing weighted sums of objectives for Pareto set generation in multicriteria optimization problems," *Structural optimization*, vol. 14, pp. 63–69, 1997.
- [11] N. Gunantara, "A review of multi-objective optimization: Methods and its applications," *Cogent Engineering*, vol. 5, no. 1, p. 1502242, 2018.
- [12] K. Qiao, J. Liang, K. Yu, M. Wang, B. Qu, C. Yue, and Y. Guo, "A self-adaptive evolutionary multi-task based constrained multi-objective evolutionary algorithm," *IEEE Transactions on Emerging Topics in Computational Intelligence*, vol. 7, no. 4, pp. 1098–1112, 2023.
- [13] D. Volpe, G. Orlandi, and G. Turvani, "Improving the solving of optimization problems: A comprehensive review of quantum approaches," *Quantum Reports*, vol. 7, no. 1, p. 3, 2025.
- [14] Z. Ye, X. Qian, and W. Pan, "Quantum topology optimization via quantum annealing," *IEEE Transactions on Quantum Engineering*, vol. 4, pp. 1–15, 2023.
- [15] F. S. Gharehchopogh, "Quantum-inspired metaheuristic algorithms: comprehensive survey and classification," *Artificial Intelligence Review*, vol. 56, no. 6, pp. 5479–5543, 2023.
- [16] Y. Li, M. Tian, G. Liu, C. Peng, and L. Jiao, "Quantum optimization and quantum learning: A survey," *Ieee Access*, vol. 8, pp. 23 568–23 593, 2020.
- [17] A. Ciacco, F. Guerriero, and G. Macrina, "Review of quantum algorithms for medicine, finance and logistics: A. ciacco et al." *Soft Computing*, vol. 29, no. 4, pp. 2129–2170, 2025.
- [18] S. Yarkoni, E. Raponi, T. Bäck, and S. Schmitt, "Quantum annealing for industry applications: Introduction and review," *Reports on Progress in Physics*, vol. 85, no. 10, p. 104001, 2022.
- [19] DWave. Hybrid Solvers for Quadratic Optimization. Accessed: 2025-07-20. [Online]. Available: <https://www.dwavequantum.com/media/soxph512/hybrid-solvers-for-quadratic-optimization.pdf>
- [20] A. Marchesin, B. Montrucchio, M. Graziano, A. Boella, and G. Mondo, "Improving urban traffic mobility via a versatile quantum annealing model," *IEEE Transactions on Quantum Engineering*, vol. 4, pp. 1–13, 2023.
- [21] A. Guillaume, E. Y. Goh, M. D. Johnston, B. D. Wilson, A. Ramanan, F. Tibble, and B. Lackey, "Deep space network scheduling using quantum annealing," *IEEE Transactions on Quantum Engineering*, vol. 3, pp. 1–13, 2022.
- [22] J. Wurtz, S. H. Sack, and S.-T. Wang, "Solving non-native combinatorial optimization problems using hybrid quantum-classical algorithms," *IEEE Transactions on Quantum Engineering*, 2024.
- [23] M. R. Bonyadi, Z. Michalewicz, and L. Barone, "The travelling thief problem: The first step in the transition from theoretical problems to realistic problems," in *2013 IEEE Congress on Evolutionary Computation*. IEEE, 2013, pp. 1037–1044.
- [24] S. Polyakovskiy, M. R. Bonyadi, M. Wagner, Z. Michalewicz, and F. Neumann, "A comprehensive benchmark set and heuristics for the traveling thief problem," in *Proceedings of the 2014 annual conference on genetic and evolutionary computation*, 2014, pp. 477–484.
- [25] Q. Zhang and H. Li, "MOEA/D: A multiobjective evolutionary algorithm based on decomposition," *IEEE Transactions on evolutionary computation*, vol. 11, no. 6, pp. 712–731, 2007.
- [26] X. Xu, S. Fu, W. Li, F. Dai, H. Gao, and V. Chang, "Multi-objective data placement for workflow management in cloud infrastructure using NSGA-II," *IEEE Transactions on Emerging Topics in Computational Intelligence*, vol. 4, no. 5, pp. 605–615, 2020.
- [27] H. Seada and K. Deb, "A unified evolutionary optimization procedure for single, multiple, and many objectives," *IEEE Transactions on Evolutionary Computation*, vol. 20, no. 3, pp. 358–369, 2015.
- [28] J. Wu, M. Wagner, S. Polyakovskiy, and F. Neumann, "Exact approaches for the travelling thief problem," in *Simulated Evolution and Learning: 11th International Conference, SEAL 2017, Shenzhen, China, November 10–13, 2017, Proceedings 11*. Springer, 2017, pp. 110–121.
- [29] A. Nikfarjam, A. Neumann, and F. Neumann, "On the Use of Quality Diversity Algorithms for the Travelling Thief Problem," *ACM Transactions on Evolutionary Learning and Optimization*, vol. 4, no. 2, pp. 1–22, 2024.
- [30] M. El Yafrani and B. Ahiod, "A local search based approach for solving the Travelling Thief Problem: The pros and cons," *Applied Soft Computing*, vol. 52, pp. 795–804, 2017.
- [31] J. Blank, K. Deb, and S. Mostaghim, "Solving the bi-objective traveling thief problem with multi-objective evolutionary algorithms," in *Evolutionary Multi-Criterion Optimization: 9th International Conference, EMO 2017, Münster, Germany, March 19–22, 2017, Proceedings 9*. Springer, 2017, pp. 46–60.
- [32] M. E. Yafrani, S. Chand, A. Neumann, B. Ahiod, and M. Wagner, "Multi-objectiveness in the single-objective traveling thief problem," in *Proceedings of the Genetic and Evolutionary Computation Conference Companion*, 2017, pp. 107–108.
- [33] J. Wu, S. Polyakovskiy, M. Wagner, and F. Neumann, "Evolutionary computation plus dynamic programming for the bi-objective travelling thief problem," in *Proceedings of the Genetic and Evolutionary Computation Conference*, 2018, pp. 777–784.
- [34] J. B. Chagas, J. Blank, M. Wagner, M. J. Souza, and K. Deb, "A non-dominated sorting based customized random-key genetic algorithm for the bi-objective traveling thief problem," *Journal of Heuristics*, vol. 27, no. 3, pp. 267–301, 2021.
- [35] D. Venturelli and A. Kondratyev, "Reverse quantum annealing approach to portfolio optimization problems," *Quantum Machine Intelligence*, vol. 1, no. 1, pp. 17–30, 2019.
- [36] T. Stollenwerk, B. O’Gorman, D. Venturelli, S. Mandra, O. Rodionova, H. Ng, B. Sridhar, E. G. Rieffel, and R. Biswas, "Quantum annealing applied to de-conflicting optimal trajectories for air traffic management," *IEEE transactions on intelligent transportation systems*, vol. 21, no. 1, pp. 285–297, 2019.
- [37] S. Kim, S.-W. Ahn, I.-S. Suh, A. W. Dowling, E. Lee, and T. Luo, "Quantum annealing for combinatorial optimization: a benchmarking study," *npj Quantum Information*, vol. 11, no. 1, p. 77, 2025.
- [38] A. Ciacco, F. Guerriero, and F. P. Saccomanno, "Quantum annealing for the two-level facility location problem," *Future Generation Computer Systems*, vol. 174, p. 107961, 2026.
- [39] P. Schworm, X. Wu, M. Klar, M. Glatt, and J. C. Aurich, "Multi-objective quantum annealing approach for solving flexible job shop scheduling in manufacturing," *Journal of Manufacturing Systems*, vol. 72, pp. 142–153, 2024.
- [40] T. V. Le, M. V. Nguyen, S. Khandavilli, T. N. Dinh, and T. N. Nguyen, "Quantum annealing approach for selective traveling salesman problem," in *ICC 2023-IEEE International Conference on Communications*. IEEE, 2023, pp. 2686–2691.
- [41] A. Ciacco, F. Guerriero, and E. Osaba, "Steiner traveling salesman problem with quantum annealing," in *Proceedings of the Genetic and Evolutionary Computation Conference Companion*, 2025, pp. 2412–2418.
- [42] A. Lucas, "Ising formulations of many NP problems," *Frontiers in physics*, vol. 2, p. 5, 2014.
- [43] T. Albash and D. A. Lidar, "Adiabatic quantum computation," *Reviews of Modern Physics*, vol. 90, no. 1, p. 015002, 2018.
- [44] A. Rajak, S. Suzuki, A. Dutta, and B. K. Chakrabarti, "Quantum annealing: An overview," *Philosophical Transactions of the Royal Society A*, vol. 381, no. 2241, p. 20210417, 2023.
- [45] S.-G. Jeong, P. D. A. Duc, Q. V. Do, D.-I. Noh, N. X. Tung, T. Van Chien, Q.-V. Pham, M. Hasegawa, H. Sekiya, and W.-J. Hwang, "Quantum Annealing-Based Sum Rate Maximization for Multi-UAV-Aided Wireless Networks," *IEEE Internet of Things Journal*, 2025.
- [46] Y. Ohkura, T. Satoh, and R. Van Meter, "Simultaneous execution of quantum circuits on current and near-future NISQ systems," *IEEE Transactions on Quantum Engineering*, vol. 3, pp. 1–10, 2022.
- [47] S. Mukherjee and B. K. Chakrabarti, "Multivariable optimization: Quantum annealing and computation," *The European Physical Journal Special Topics*, vol. 224, no. 1, pp. 17–24, 2015.
- [48] K. K. Mishra and S. Harit, "A fast algorithm for finding the non dominated set in multi objective optimization," *International*

- Journal of Computer Applications, vol. 1, no. 25, pp. 35–39, 2010.
- [49] C. Bu, F. Liu, Z. Cao, L. Li, Y. Zhang, X. Hu, and W. Luo, “Cognitive diagnostic model made more practical by genetic algorithm,” *IEEE Transactions on Emerging Topics in Computational Intelligence*, vol. 7, no. 2, pp. 447–461, 2022.
 - [50] J. Blank and K. Deb, “Pymoo: Multi-objective optimization in python,” *Ieee access*, vol. 8, pp. 89 497–89 509, 2020.
 - [51] N. Riquelme, C. Von Lüken, and B. Baran, “Performance metrics in multi-objective optimization,” in *2015 Latin American computing conference (CLEI)*. IEEE, 2015, pp. 1–11.